Structure of 1-Naphthol−Water Clusters Studied by IR Dip Spectroscopy and Ab Initio Molecular Orbital Calculations

Ruriko Yoshino,[†] Kenro Hashimoto,[‡] Takuichiro Omi,[†] Shun-ichi Ishiuchi,[§] and Masaaki Fujii*[,§]

Department of Chemistry, Graduate School of Science and Engineering, Waseda University/PRESTO-JST, Ohkubo, Shinjuku-ku, Tokyo 169-8555, Japan, Computer Center, Tokyo Metropolitan University, 1-1 Minami-Ohsawa, Hachioji, Tokyo, 192-0397 Japan, and Institute for Molecular Science, Myodaiji, Okazaki 444-8585, Japan

Received: March 16, 1998; In Final Form: May 12, 1998

The IR spectrum of *cis*-1-naphthol, *trans*-1-naphthol, and 1-naphthol·$(H_2O)_n$ ($n = 1-3$) clusters has been measured by the IR dip spectroscopy in a supersonic jet. The spectra show clear vibrational structures of the monomers and the clusters in the energy region from 3000 to 3800 cm^{-1}. Observed vibrational transitions are assigned to the OH stretching vibrations of 1-naphthol and waters in the clusters. The size dependence of the IR bands and the cluster geometries are analyzed by using the ab initio MO method at the MP2/6-31G level. From the comparison between the observed and calculated IR spectra, we have concluded that the 1-naphthol acts as the proton donor and a cyclic hydrogen-bond network is formed in the $n = 2$ and 3 clusters.

I. Introduction

Solvated phenol and naphthols have attracted many workers because of their proton-transfer reaction in the excited electronic state.[1−3] This photoinduced proton transfer was first observed in the fluorescence spectrum in aqueous solution and has been discussed in connection with the increase in acidity after the electronic excitation. Among these molecules, 1-naphthol shows the most drastic change: its pK_a decreases to 0.5 from 9.1 in going from S_0 to S_1.[2] Therefore, it is expected that 1-naphthol is one of the most ideal molecules to study photoinduced proton-transfer reactions, and various approaches have been reported.[4−6]

Recently, the microscopic nature of the solution has been studied actively by using laser spectroscopy to study solute−solvent clusters.[7−11] For aqueous 1-naphthol, Leutwyler's group has applied mass-selected multiphoton ionization (MPI) spectroscopy to 1-naphthol·$(H_2O)_n$ ($n = 1-50$) clusters and determined the origins of the S_1-S_0 transition.[7,8] The dispersed fluorescence spectrum, ionization threshold spectrum, and picosecond decay have also been measured for these systems.[8−10] The most significant result in this work is the size dependence of the proton transfer reaction. The reaction proceeds only in the clusters including more than 30 water molecules. Though this fact has been discussed in terms of the stabilization of the polar electronic state ^1L_a by the hydration,[8] a definite explanation has not been established yet.

To understand the mechanism of the size-dependent proton-transfer reaction, the cluster structure in S_1, i.e., the initial conformation of the reaction, is indispensable information. The geometry in S_0 is as important as that in S_1 because the electronically excited clusters are prepared by a vertical optical transition. Nevertheless, the conformation of the clusters is not well-known, not only in the reactive S_1 state but also in the ground-state S_0 except for the 1-naphthol·$(H_2O)_2$ cluster.[11] Its structure has been determined by rotational coherence spectroscopy; however, no further application has been reported. On the other hand, several structures of 1-naphthol·$(H_2O)_n$ have been obtained for n up to 4 from semiemperical calculations.[9] However, there has been no theoretical report that discusses the spectroscopic observables on the basis of the calculated structures. Thus, for a better understanding of the cluster structures, it is essential to compare observed and calculated spectra.

In this work, we investigate the structures of aqueous 1-naphthol clusters in S_0 by vibrational spectroscopy combined with ab initio MO calculations. The key vibrations to characterize the structures are the OH stretching modes. Their frequencies sensitively reflect the hydrogen bond in aqueous clusters. We observe the OH stretching vibrations by IR dip spectroscopy, which measures IR transitions for a specific cluster by the IR−UV double resonance process. Simultaneously, ab initio MO calculations at the correlated level are applied to each cluster, and the IR spectra are predicted for various stable conformations. From the comparison between the observed and calculated IR spectra, the vibrational assignments and the structures of the 1-naphthol·$(H_2O)_n$ ($n = 0-3$) are discussed.

II. Methods

A. Experimental Method. The IR spectra of the *cis*- and *trans*-1-naphthol monomers and 1-naphthol·$(H_2O)_n$ ($n = 1-3$) clusters are measured by IR dip spectroscopy. This method and other IR depletion techniques have been applied to the vibrational spectroscopy of jet-cooled molecules, clusters, and ion clusters.[12−28] The principle of the IR dip spectroscopy is shown in Figure 1. The IR laser (ν_{IR}) irradiates the sample in a supersonic jet scanning in the energy region from 3000 to 3800 cm^{-1}, while a UV laser (ν_{UV}) ionizes the molecule in the ground vibrational state by the resonant-enhanced two-photon ionization via the S_1 state. When the frequency of the IR laser matches the transition to a certain vibrational level, the ion

* To whom correspondence should be addressed. Fax: +81-564-54-2254. E-mail: mfujii@ims.ac.jp.
[†] Waseda University/PRESTO-JST.
[‡] Tokyo Metropolitan University.
[§] Institute for Molecular Science.

S1089-5639(98)01500-X CCC: $15.00
Published on Web 07/15/1998

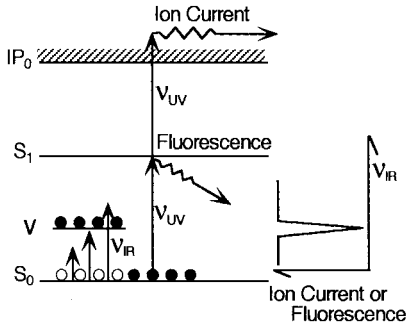

Figure 1. Principle of IR dip spectroscopy.

current decreases because of the loss of population from the ground vibrational state. As a result, the vibrational transition is detected as a depletion of the ion current (ion-detected IR dip spectroscopy). The same spectrum can be obtained when the fluorescence intensity from S_1 is monitored instead of the ion current (fluorescence-detected IR dip spectroscopy).

Ion-detected IR dip spectroscopy has an advantage by detecting the mass-selected ion with a mass filter. Therefore, the ion current was monitored to obtain the IR dip spectra of *trans*-1-naphthol monomer and 1-naphthol·$(H_2O)_n$ ($n = 1, 2$) clusters. However, ion-detected IR spectroscopy is difficult to apply when the ionization efficiency is low. For this reason, the fluorescence from S_1 was monitored to obtain the spectrum of *cis*-1-naphthol monomer. Also, the spectrum of the 1-naphthol·$(H_2O)_3$ cluster was measured by monitoring the fluorescence from S_1 because of the weak mass-selected ion signal due to the collisional dissociation of the cluster after ionization in our experimental setup.

A detailed description of the experimental setup for ion-detected IR dip spectroscopy is presented elsewhere.[29] Briefly, the second harmonic of the Nd^{3+}:YAG laser (Continuum Surelite II) and the output of a dye laser (Lumonics HD-500) pumped by the second harmonic of the YAG laser were differentially mixed in a $LiNbO_3$ crystal to generate tunable IR. The UV radiation was generated with a KDP crystal (Inrad, Autotracker II) by the frequency-doubling of a second dye laser (Lumonics HD-500) pumped by the third harmonic of another YAG laser (Lumonics YM-1200). Both the IR laser and the UV laser were coaxially introduced into a vacuum chamber (Toyama/Hakuto) and crossed a supersonic jet. The IR laser irradiated the sample prior to the UV laser by 50 ns. The timing between the two lasers was adjusted by a digital delay generator (Stanford Research DG-535). The molecules or clusters ionized by the UV laser were detected by a channel multiplier (Murata Ceratron) through a quadrupole mass filter (Extrel). The signal was amplified by a preamplifier (EG&G PARC model 115) and was integrated by a digital boxcar (EG&G PARC model 4420/4422). The integrated signal was recorded by a personal computer (NEC PC 9801) as a function of IR laser frequency.

The experimental configuration for the fluorescence-detected IR dip spectroscopy is the same as for the ion-detected IR dip spectroscopy expect for the fluorescence detection system. The fluorescence from the sample was collected by a lens and detected by a photomultiplier (Hamamatsu 1P28) through filters (Toshiba UV-35 and Corning 7-54).

Naphthol vapor at 353 K was seeded in He gas at 2 atm, which contained water vapor at 268−278 K. The mixture was then expanded into the vacuum chamber through a pulsed nozzle operated at 20 Hz. Naphthol was purchased from Tokyo Kasei and was used after purification.

B. Calculation. Molecular structures of *trans*-1-naphthol, *cis*-1-naphthol, and *trans*-1-naphthol·$(H_2O)_n$ ($n = 1-3$) were optimized by using an energy gradient technique for the second-order many-body perturbation method (MP2)[30] with the usual frozen core approximation. The basis set used was the standard 6-31G basis set.[31,32] Vibrational analysis using the analytical second-derivative matrix was carried out to characterize the nature of the stationary points. If the optimized structure has one or more imaginary frequencies, we further optimized the structure until the true local minimum structure was obtained, where all the vibrational frequencies are real. The IR intensities for the vibrations are evaluated for all minimum structures. The total hydration enthalpies at 0 K were computed with the calculated harmonic frequencies without scaling. The program used was Gaussian 94.[33]

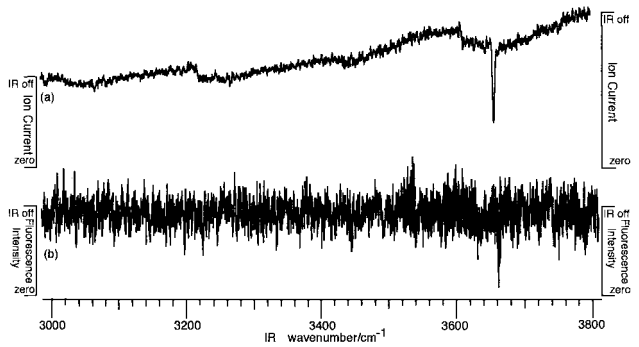

Figure 2. IR dip spectra of (a) *trans*-1-naphthol and (b) *cis*-1-naphthol.

III. Results and Discussion

A. IR Dip Spectra of Monomers. Prior to the study of the clusters, the IR spectrum of the 1-naphthol monomer should be discussed briefly. Two rotational isomers are possible for 1-naphthol:

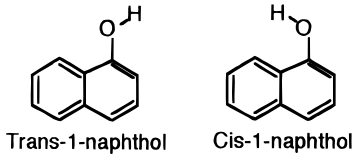

Trans-1-naphthol Cis-1-naphthol

From the high-resolution fluorescence excitation spectrum, the origin of the S_1-S_0 electronic transition was assigned for each species.[34] However, the stretching vibrations of the OH group, which distinguish the isomer from the other, have not been observed.

Figure 2a shows the ion-detected IR dip spectrum of *trans*-1-naphthol monomer obtained when the UV laser was fixed to its S_1 origin (31 457 cm^{-1}).[7,8] The zero level (zero) and the ion signal without ν_{IR} (IR off) are indicated by solid lines besides the spectrum. The baseline of the spectrum varies because of the variation of the UV laser power. The ion current clearly decreases when the IR laser reaches 3655 cm^{-1}. From its frequency, the dip is assigned to the OH stretching vibration (ν_{OH}) of *trans*-1-naphthol. Other vibrational transitions such as CH stretching modes were not observed. Figure 2b shows the fluorescence-detected IR dip spectrum of *cis*-1-naphthol monomer obtained when the UV laser was fixed to its S_1 origin (31 181 cm^{-1}).[34] The spectrum shows a single dip at 3663 cm^{-1}, which corresponds to ν_{OH} of the cis isomer.

Both the trans and the cis isomers show similar IR dip spectra, with only a single IR transition appearing in the region from 3000 to 3800 cm^{-1}. However, the vibrational frequency of ν_{OH} in the trans isomer is different from that of the cis by 8 cm^{-1}.

TABLE 1: Observed and Calculated OH Stretching Frequencies (cm^{-1}) of 1-Naphthol Monomers and 1-Naphthol·$(H_2O)_n$ (n = 1−3) Clusters and Water Monomer

	observed frequencies			calculated frequencies		
		water moiety			water moiety	
	1-naphthol ν_{OH}	H-bonded OH stretch	non-H-bonded OH stretch	1-naphthol ν_{OH}	H-bonded OH stretch	non-H-bonded OH stretch
cis-1-naphthol	3663			3651		
trans-1-naphthol	3655			3640		
1-naphthol·$(H_2O)_1$	3507		3746[c]	3434	3687[b]	3852[c]
1-naphthol·$(H_2O)_2$	3370	3499	3720	3215	3429	3809
		3559			3535	3814
1-naphthol·$(H_2O)_3$	3205	3347	3715	2976	3186	3809
		3429	3725		3296	3811
		3468			3404	3817
H_2O[a]		3657[b]	3756[c]		3657[b]	3833[c]

[a] Energy of $J = 0$, $K = 0$ level. Reference 36. [b] OH symmetric stretching mode ν_1. [c] OH antisymmetric stretching mode ν_3.

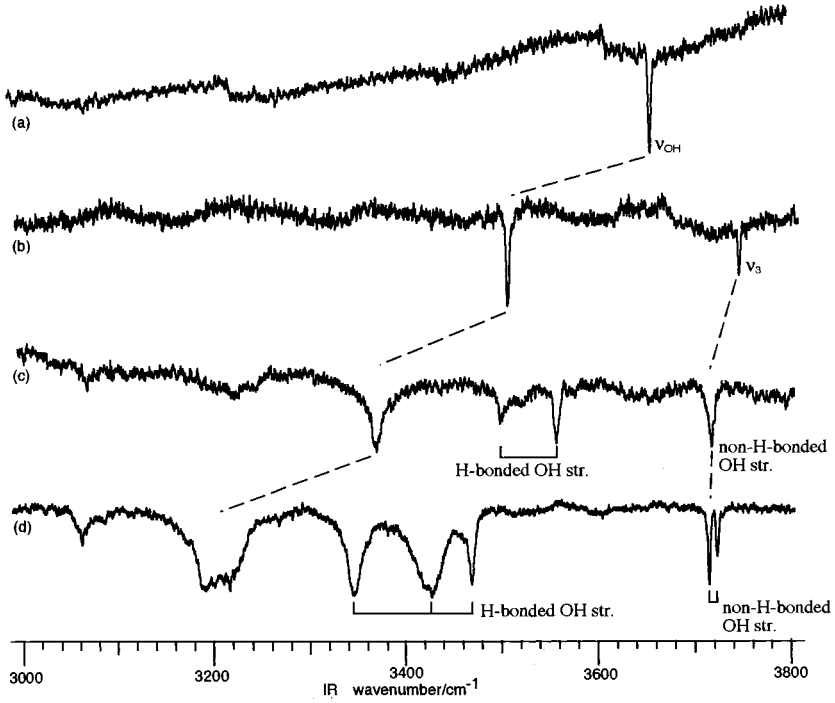

Figure 3. IR dip spectra of (a) *trans*-1-naphthol, (b) 1-naphthol·$(H_2O)_1$, (c) 1-naphthol·$(H_2O)_2$, and (d) 1-naphthol·$(H_2O)_3$.

The difference in vibrational frequency reconfirms the existence of the two rotational isomers in a supersonic jet.

B. IR Dip Spectra of Clusters. As we have demonstrated in the previous section, IR dip spectroscopy can measure the vibrational transitions of a specific species by choosing the frequency of the UV laser. In this section, we show the IR dip spectra of clusters consisting of the trans isomer and water molecules. The IR dip spectra of 1-naphthol·$(H_2O)_n$ (n = 1−3) are shown in parts b−d of Figure 3, respectively. The IR dip spectrum of the *trans*-1-naphthol monomer is also shown in Figure 3a for comparison. All the spectra are obtained by fixing the UV laser to the S_1 origin of each species, which are 31 314, 31 373, and 31 321 cm^{-1} for 1-naphthol·$(H_2O)_n$ (n = 1−3), respectively.[7,8]

The IR dip spectrum of 1-naphthol·$(H_2O)_1$ cluster shows two dips at 3507 and 3746 cm^{-1} (see Figure 3b). From their frequencies, they are assignable to the OH stretching vibrations in the cluster. There are three OH stretching vibrational modes in this cluster: the OH stretching vibration of the 1-naphthol (ν_{OH}) and the symmetric and the antisymmetric vibrations of the water (ν_1 and ν_3, respectively). Here, we tentatively assign the observed bands by assuming that the 1-naphthol is a proton donor in the cluster. Since the frequency of the OH stretching vibration of the proton donor is known to decrease in solution and hydrogen-bonded clusters,[13−19,35] the band at 3507 cm^{-1} is assigned to ν_{OH}. The band at 3746 cm^{-1} is close to ν_3 in a free water molecule[36] and is therefore assigned to ν_3 of the water moiety in the cluster. It should be noted that ν_1 is not observed in the spectrum, as its oscillator strength is less than $^1/_{10}$ at the ν_3 mode in a free water molecule.[36]

Parts c and d of Figure 3 show the IR dip spectra of 1-naphthol·$(H_2O)_2$ and 1-naphthol·$(H_2O)_3$, respectively. The 1-naphthol·$(H_2O)_2$ cluster shows four bands, while 1-naphthol·$(H_2O)_3$ shows six strong bands in the region from 3200 to 3700 cm^{-1}. Because of their frequencies, the bands should also be assigned to OH stretching vibrations. The band at the lowest frequency (3370 and 3205 cm^{-1} for n = 2 and 3, respectively) is tentatively assigned to ν_{OH} in each cluster. The bands lying in the region higher than ν_{OH} of the monomer (3720 cm^{-1} for n = 2; 3715 and 3725 cm^{-1} for n = 3) are assigned to a stretching vibration of the free OH bond of the water moieties in the clusters (non-H-bonded OH stretch). Consequently, the bands between ν_{OH} and the non-H-bonded OH stretch (at 3499 and 3559 cm^{-1} for n = 2; at 3347, 3429, and 3468 cm^{-1} for

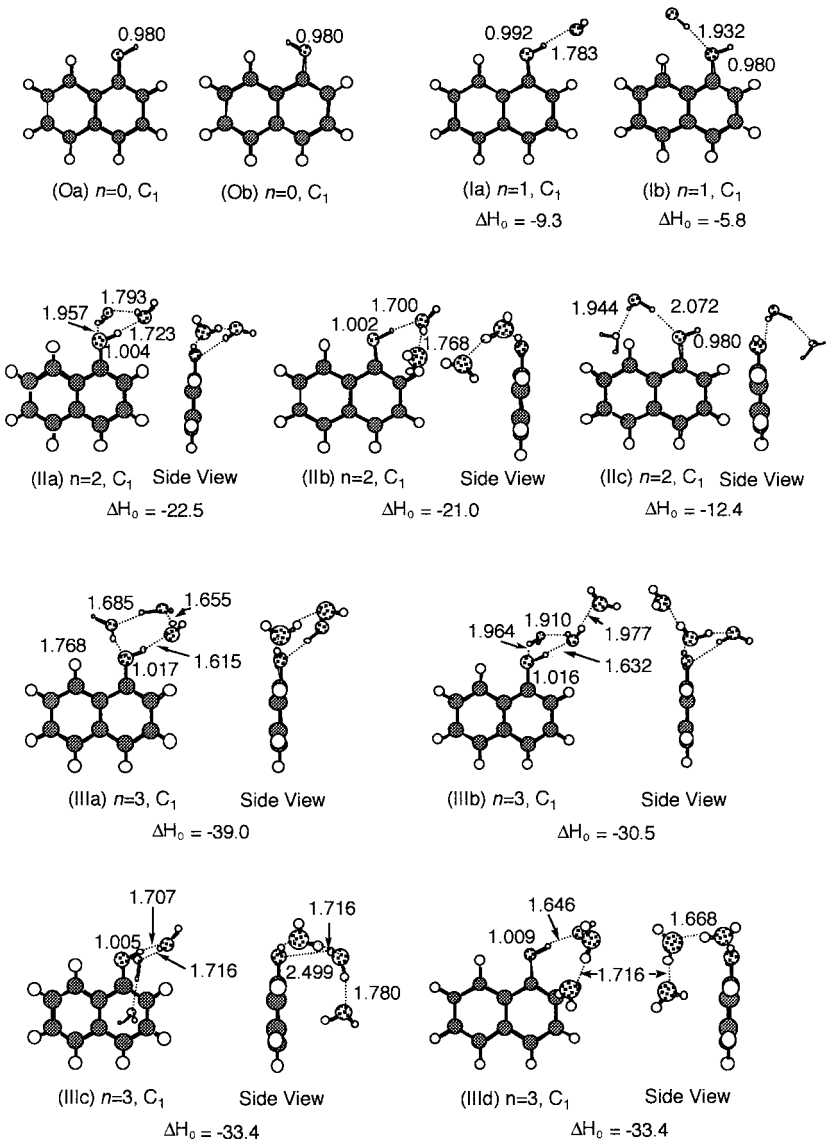

Figure 4. Optimized structures of 1-naphthol·$(H_2O)_n$ ($n = 0-3$) at MP2/6-31G level. Naphthol OH and hydrogen bond distances are given in angstroms. Molecular symmetries and calculated total hydration enthalpies at 0 K (ΔH_0) are also presented in kcal/mol.

$n = 3$) are assigned to a stretching vibration of hydrogen-bonded OH group of the water moieties in the clusters (H-bonded OH stretch). In addition, a weak feature at 3066 cm^{-1} is observed in the spectrum of 1-naphthol·$(H_2O)_3$ cluster. From its frequency, it is tentatively assigned to the CH stretching vibration of the 1-naphthol in the cluster. Frequencies of the observed OH vibrations in the clusters are listed in Table 1.

C. Assignment of the Bands and Structures of *trans*-1-Naphthol·$(H_2O)_n$ ($n = 1-3$). In this section, we examine the assignment of the bands in the IR dip spectra and discuss the structures of *trans*-1-naphthol·$(H_2O)_n$ ($n = 1-3$) clusters based on ab initio MO calculations. The optimized geometries of the *trans*- and *cis*-1-naphthol and *trans*-1-naphthol·$(H_2O)_n$ ($n = 0-3$) are shown in Figure 4. The *trans*-1-naphthol (**Oa**) is more stable than the cis isomer (**Ob**) by 2.1 kcal/mol including zero-point vibrational corrections. The calculated ν_{OH} are 3640 (trans) and 3651 (cis) cm^{-1}, both of which are in good agreement with the experimental results.

For the $n = 1$ cluster, we have found two isomers: **Ia** and **Ib**. In structure **Ia**, the 1-naphthol is a proton donor and there remain two free OH groups in the water part. On the other hand, the 1-naphthol is a proton acceptor in **Ib**. The water molecule is bound to the 1-naphthol molecule by a single hydrogen bond, and both 1-naphthol and water molecules have free OH groups in this complex. The calculated total hydration enthalpy at 0 K for **Ia** is −9.3 kcal/mol, while that for **Ib** is −5.8 kcal/mol. Thus, the former is expected to be more abundant than the latter in the supersonic jet.

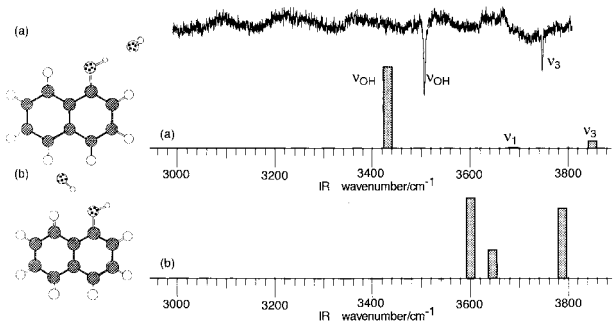

Figure 5. Calculated IR spectra of 1-naphthol·$(H_2O)_1$ for the optimized structures (a) **Ia** and (b) **Ib**. The structures **Ia** and **Ib** are illustrated to the side of the calculated spectra. The observed IR dip spectrum is also shown on top.

The calculated IR spectra for **Ia** and **Ib** are shown in Figure 5, together with the observed spectrum. The harmonic frequen-

cies of the ν_1 and ν_3 bands for the isolated water molecule were computed to be 3657 and 3833 cm^{-1}, respectively. In the spectrum for **Ia**, there are one strong and two weak bands at 3434, 3687, and 3852 cm^{-1}. Their relative IR intensities are 1.00, 0.01, and 0.09, respectively. The calculated normal mode corresponding to the band at 3434 cm^{-1} is mostly the OH stretching of the 1-naphthol, and those for the two higher bands are mainly the symmetric (3687 cm^{-1}) and asymmetric (3852 cm^{-1}) stretching vibrations of the OH bonds in the water. Thus, we can regard these bands as ν_{OH}, ν_1, and ν_3 bands in this order. The ν_{OH} band is red-shifted due to the proton donation of the OH group in the hydrogen bond. On the other hand, the frequencies of ν_1 and ν_3 have remained almost unchanged from those of the free water, and ν_1 is much weaker than ν_3. These facts indicate that the vibrational nature of the water is not so affected in the complex. In addition, the water bands are much weaker than the ν_{OH} band. In the spectrum for **Ib**, we also see three bands whose relative intensities are 1.00, 0.35, and 0.87, respectively. Their normal modes are the vibrations of the hydrogen-bonded water OH (3602 cm^{-1}), the naphthol OH (3646 cm^{-1}), and the free water OH (3787 cm^{-1}). The ν_{OH} band is located between the water bands, and its red shift by the hydration is only 6 cm^{-1}, since the naphthol OH bond is free from the hydrogen bond in **Ib**. It is interesting to note that the water bands are calculated to be more intense than the ν_{OH} band, and we expect three bands of comparable intensity for this complex. By comparing the two calculated spectra with the experimental one, we can easily note that the observed spectrum is better reproduced by **Ia** than by **Ib**, especially from the number of bands, though ν_1 is unobserved with the present signal-to-noise ratio in the IR dip spectrum. The calculated frequency of ν_{OH} underestimates the experiment only by 2% and that of ν_3 overshoots by 3%. Therefore, we have concluded that the observed spectrum can be attributed to the structure where 1-naphthol is a proton donor, and we have confirmed the tentative assignment of the observed bands in the previous section.

The optimized structures for the $n = 2$ clusters are **IIa**−**IIc** in Figure 4. In structure **IIa**, the 1-naphthol acts not only as a proton-donor but also as a proton acceptor. Indeed, each component molecule in this cluster donates one OH group to a hydrogen bond while accepting an OH group from another, resulting in a six-membered ring formed by the hydrogen-bond network. We can call this a "cyclic" structure. On the other hand, the complexes **IIb** and **IIc** are "chain" structures in which a water dimer is bound to the 1-naphthol by one of the oxygen atoms through a single hydrogen bond. The 1-naphthol molecule is the proton donor in **IIb**, while it is the proton acceptor in **IIc**. The calculated total hydration enthalpies are −22.5, −21.0, and −12.4 kcal/mol from **IIa** to **IIc**, respectively. The "cyclic" form is more stable than the "chain" isomers.

The theoretical IR spectra of the **IIa**−**IIc** structures are shown in Figure 6 together with the observed IR dip spectrum for *trans*-1-naphthol·$(H_2O)_2$. We note that the calculated spectra for **IIa** agrees with the experimental results much better than others. Experimentally, we have observed four dips at 3370, 3499, 3559, and 3720 cm^{-1}. The calculated frequencies of the OH vibrations for **IIa** are 3215, 3429, 3535, 3809, and 3814 cm^{-1}, but we see the two highest bands are overlapping in the spectrum. The structure **IIb** shows two strong and three weak bands. The relative intensities of the third and fourth bands are quite different from those of the observed spectrum. On the other hand, the calculated lowest frequency among the OH vibrations for **IIc** is much larger than the observed one. This structure

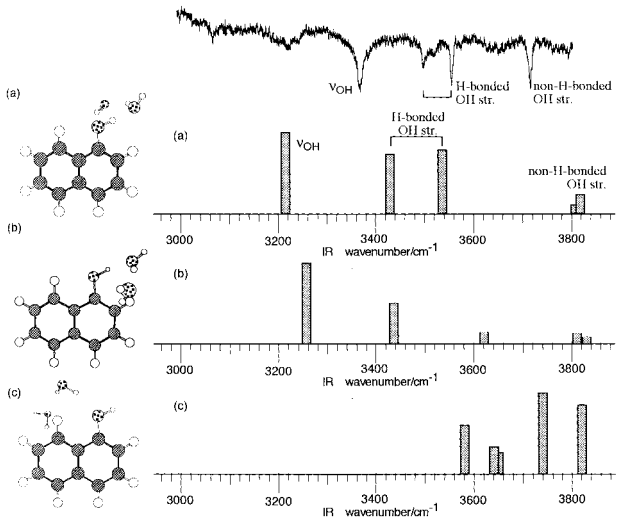

Figure 6. Calculated spectra of 1-naphthol·$(H_2O)_2$ for the optimized structures (a) **IIa**, (b) **IIb**, and (c) **IIc**. The structures **IIa**−**IIc** are illustrated to the side of the calculated spectra. The observed IR dip spectrum is also shown on top.

explains neither the positions nor the splitting of the bands. Therefore, we should rule out the structures **IIb** and **IIc**. The calculated normal modes of the three low bands for **IIa** are the vibrations of the hydrogen-bonded OH bonds in the cycle, and the vibration of the naphthol OH is almost a dominant contributor to the lowest one. So we can call the band at 3215 cm^{-1} the ν_{OH} and the other two at 3429 and 3535 cm^{-1} the H-bonded OH stretch. On the other hand, the normal modes for the two higher bands at 3809 and 3814 cm^{-1} are vibrations associated with the free water OH group extending out of the ring. These are the non-H-bonded OH stretch bands. It is worth emphasizing that these modes are no longer the pure symmetric and asymmetric OH stretching vibrations of each water "molecule" but the vibrations of the "cluster". For example, the vibrational motions of the H-bonded OH stretch are the deformation of the hydrogen-bonded ring structure in a sense. Quantitatively speaking, the calculation underestimates the frequencies of ν_{OH} and the H-bonded OH stretch at most by 5%, while it overshoots those of non-H-bonded OH stretch by around 3%. The ν_{OH} band is further shifted to the red from $n = 1$ by ∼220 cm^{-1}, while the decreases of the frequencies of the non-H-bonded OH stretch from the pure water ν_3 are only ∼40 cm^{-1}. As a summary, we have concluded that the 1-naphthol·$(H_2O)_2$ cluster has the "cyclic" form and have confirmed the tentative assignments of the observed bands in the previous section. This cyclic structure is also consistent with the result from rotational coherence spectroscopy.[11]

For the $n = 3$ cluster, the number of potential minimum configuration is expected to be large. However, since we have learned that the number of observed bands from ∼3300 to ∼3600 cm^{-1} can be probably related to the number of hydrogen-bonded OH groups of water, we have narrowed our focus mainly to the "cyclic" structures with three water OH bonds in the hydrogen bond network. The optimized geometries of the cyclic forms are **IIIa**−**IIIc** in Figure 4. Their calculated total binding enthalpies are −39.0, −30.5, and −33.4 kcal/mol from **IIIa** to **IIIc**, respectively. In the structure **IIIa**, all component molecules donate OH groups to hydrogen bonds and there is an eight-membered ring. On the other hand, the complexes **IIIb** and **IIIc** can be regarded as the structures where the third water molecule is bound to the cyclic **IIa** in the outer shell. The newly formed hydrogen bond from $n = 2$ to $n = 3$ is included in the

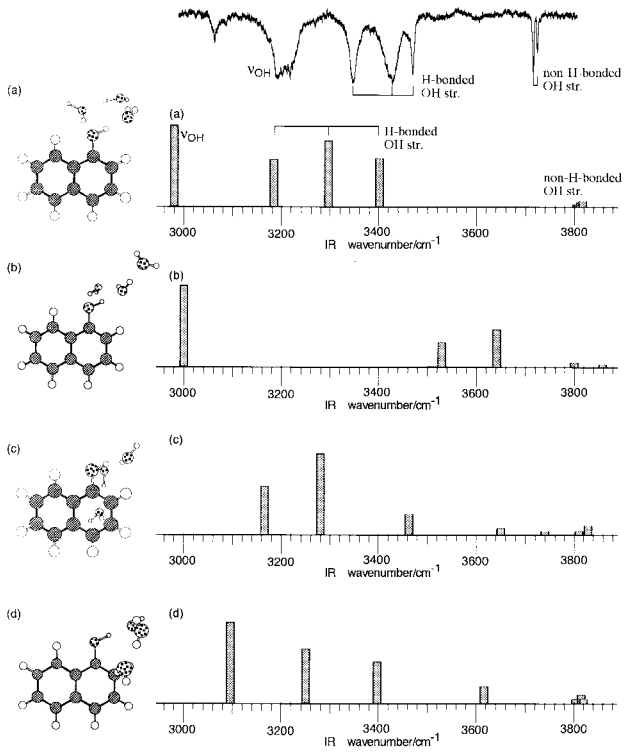

Figure 7. Calculated spectra of 1-naphthol·$(H_2O)_3$ for the optimized structures (a) **IIIa**, (b) **IIIb**, (c) **IIIc**, and (d) **IIId**. The structures **IIIa**−**IIId** are illustrated to the side of the calculated spectra. The observed IR dip spectrum is also shown on top.

ring in **IIIa**, while it is out of the ring in **IIIb** and **IIIc**. In addition, we have obtained the "chain" structure **IIId** for comparison. It is less stable than **IIIa** by 5.6 kcal/mol. Though we have tried to find the structure where a water trimer is bound to the 1-naphthol, the geometry optimization finally converged to the structure **IIIa** or **IIId**.

The calculated IR spectra for the four structures are shown in Figure 7. This figure indicates clearly that the structure **IIIa** is the best candidate among the isomers examined for the observed IR dip spectrum for $n = 3$. Only **IIIa** shows the four strong and one weak bands near the observed dips. In addition, the absence of the bands between ∼3500 and ∼3700 cm^{-1} is also well reproduced only by this complex. As expected from the structure, the frequencies of the free OH vibrations are calculated to be almost degenerate (3809, 3811, and 3817 cm^{-1}) and their intensities are 0.03, 0.06 and 0.08 relative to the lowest band. Since only two dips have been observed around 3720 cm^{-1}, we might expect the first two bands to overlap. However, we cannot analyze these bands further because of the resolution of the spectrum and the difficulty of discussing such small differences in the frequencies and IR intensities at the present level of calculation. The remaining four bands correspond to the vibrations of the hydrogen-bonded OH groups in the ring. The vibration of the naphthol OH bond is coupled with those of the other water OH bonds in the cycle to some extent particularly in the two lowest bands, but it is the largest contributor to the normal mode of the lowest band. So the lowest band (2976 cm^{-1}) can be regarded as the naphthol OH vibration modified by hydration, and the three middle bands are the vibrations of the hydrogen-bonded water OH groups forming the ring structure. Therefore, we can assign the observed strong band at 3205 cm^{-1} to ν_{OH} , the next three bands to the H-bonded OH stretch, and the last two bands to a non-H-bonded OH stretch by following the discussion for $n = 2$. The calculated frequency of ν_{OH} is lower than the observed by 7%, while the other theoretical OH frequencies differ from the experimental value at most by 5%. We note that the difference between the observed and calculated frequencies of ν_{OH} in 1-naphthol·$(H_2O)_n$ increases as n grows, which is similar to those in phenol·$(H_2O)_n$.[37] The ν_{OH} of the 1-naphthol·$(H_2O)_3$ is calculated to be lower than the CH vibrations; seven bands with intensities less than 0.01 are calculated at 3212−3161 cm^{-1} for CH vibrations. It is certainly a large underestimation of the ν_{OH} frequency. From the energy relationship among isomers and their vibrational spectral features, we have concluded that the 1-naphthol·$(H_2O)_3$ is the cyclic structure (**IIIa**) having the eight-membered ring. All observed and calculated frequencies of the OH vibrations and their assignments are summarized in Table 1.

IV. Conclusion and Future Work

The IR spectra of the 1-naphthol·$(H_2O)_n$ ($n = 0-3$) clusters have been observed by IR dip spectroscopy for the first time. All the spectra show clear vibrational structures because of the hydrogen-bonded OH stretching modes in the clusters. The observed IR spectra are compared with the theoretical spectra of the various stable conformations predicted by ab initio MO calculations. From the comparison, the vibrational assignments and the geometrical structures of the clusters in the ground state are determined; only the most stable structures for each n reproduce the correct spectral patterns.

We can classify the observed bands of 1-naphthol·$(H_2O)_n$ into three groups, especially for $n \geq 2$. The first group is for the ν_{OH} band, which always appears at the lowest frequency among the OH bands. This band is red-shifted by 137−165 cm^{-1} for each successive water, and the decrease in frequency corresponds roughly to the elongation of the naphthol OH bond (see Figure 4 and Table 1). The second is the non-H-bonded OH stretch group for the bands of the free OH vibrations, whose frequencies are over 3700 cm^{-1}. The shift of the bands in this group with stepwise hydration is much smaller than that of the ν_{OH} band, since they are "free" from the hydrogen bonds. The third is the H-bonded OH stretch group for $n \geq 2$, bracketed between the ν_{OH} and the non-H-bonded OH stretch groups. Since the hydration structure where 1-naphthol acts not only as the proton donor but also as the proton acceptor is more stable than others with the same n, the 1-naphthol·$(H_2O)_n$ species tend to have cyclic forms to maximize the number of hydrogen bonds. This trend continues at least till $n = 3$. Therefore, the appearance of the bands in this group indicates the formation the cyclic ring structure, and the number of the bands is coincident with the hydrogen-bonded OH in the ring. The spectral feature summarized above is similar to that of phenol·$(H_2O)_n$ in which the cyclic hydrogen-bonded conformation is concluded for $n = 2$ and 3.[13,15,32] It should also be noted that the "cyclic" conformation is found in other OH-hydrogen-bonded clusters, such as pure water clusters,[38,39] aqueous Cs^+ clusters,[26] and phenol trimers.[40]

From the geometry in S_0, the structure in the excited state can be estimated roughly. In the S_1-S_0 electronic spectrum of the clusters, the transition intensity concentrates in the S_1 origin and intermolecular vibrations are not prominent.[7,8] The intensity distribution suggests that the electronically excited clusters have structures similar to those in S_0. Therefore, the 1-naphthol·$(H_2O)_{2,3}$ cluster is expected to hold the cyclic conformation also in the S_1 state. It is consistent with the small reactivity of the proton transfer in these clusters. The proton transfer is thought to occur only if the polar ^1L_a $\pi\pi^*$ state is lowered more than

the optically active S_1 $\pi\pi^*$ state by the solvation.[8] In the cyclic conformation, the π and π^* orbitals are not perturbed strongly because the water molecules are located far from the aromatic ring. This small perturbation does not alter the energy order of the $\pi\pi^*$ states; therefore, the proton transfer is not expected to take place. The detailed mechanism will become clear if the structure of the electronically excited cluster is determined directly. For this purpose, vibrational spectroscopy and the theoretical calculations should be applied to the clusters in the S_1 state. The vibrational spectroscopy of reactive clusters, such as large hydrated naphthol clusters or the naphthol solvated by ammonia molecules, will be important in establishing the mechanism of the proton-transfer reaction. These projects are now in progress.

Acknowledgment. We thank Professor James M. Lisy of the University of Illinois for reading the manuscript and making a number of helpful suggestions during his stay at the Institute for Molecular Science. This work was financially supported in part by a Grants-in-Aid from the Ministry of Education, Science, Sports and Culture, Japan. All computations were carried out at the computer centers at Tokyo Metropolitan University and Institute for Molecular Science.

References and Notes

(1) Bartok, W.; Lucchesi, P. J.; Snider, N. S. *J. Phys. Chem*. **1961**, *84*, 1842.
(2) Harris, C. M.; Sellnger, B. K. *J. Phys. Chem*. **1980**, *84*, 1366.
(3) Harris, C. M.; Sellnger, B. K. *J. Phys. Chem*. **1980**, *84*, 891.
(4) Webb, S. P.; Philips, L. A.; Yeh, S. W.; Tolbert, L. M.; Clark, J. H. *J. Phys. Chem*. **1986**, *90*, 5154.
(5) Krshnan, R.; Fillingim, T. G.; Lee, J.; Robinson, G. W. *J. Am. Chem. Soc*. **1990**, *112*, 1353.
(6) Pines, E.; Fleming, G. R. *Chem. Phys.* **1994**, *183*, 393.
(7) Knochenmuss, R.; Cheshnovsky, O.; Leutwyler S. *Chem. Phys. Lett.* **1988**, *144*, 317.
(8) Knochenmuss, R.; Leutwyler, S. *J. Chem. Phys*. **1989**, *91*, 1268.
(9) Kim, S. K.; Li, S.; Bernstein, E. R. *J. Chem. Phys*. **1991**, *95*, 3119.
(10) For a review, see the following. Kim, S. K.; Breen, J. J.; Willberg, D. M.; Heikal, A.; Syage, J. A.; Zewail, A. H. *J. Chem. Phys.* **1995**, *99*, 7421 and references therein.
(11) Connell, L. L.; Ohline, S. M.; Joireman, P. W.; Felker, P. M. *J. Chem. Phys.* **1990**, *94*, 4668.
(12) Page, P. H.; Shen, Y. R.; Lee, Y. T. *J. Chem. Phys.* **1988**, *88*, 5362.
(13) Tanabe, S.; Ebata, T.; Fujii, M.; Mikami, N. *Chem. Phys. Lett.* **1993**, *215*, 347.
(14) Iwasaki, A.; Fujii, A.; Watanabe, T.; Ebata, T.; Mikami, N. *J. Phys. Chem*. **1996**, *100*, 16053.
(15) Watanabe, T.; Ebata, T.; Tanabe, S.; Mikami, N. *J. Chem. Phys*. **1996**, *105*, 408.
(16) Pribble, R. N.; Zwier, T. S. *Science*. **1994**, *265*, 75.
(17) Pribble, R. N.; Zwier, T. S. *Faraday Discuss.* **1994**, *97*, 229.
(18) Pribble, R. N.; Garrett, A. W.; Haber, K.; Zwier, T. S. *J. Chem. Phys*. **1995**, *103*, 531.
(19) Fredericks, S. Y.; Jordan, K. D.; Zwier, T. S. *J. Phys. Chem*. **1996**, *100*, 7810.
(20) Riehn, Ch.; Lahmann, Ch.; Wassermann, B.; Brutschy, B. *Chem. Phys. Lett.* **1992**, *197*, 443.
(21) Riehn, Ch.; Lahmann, Ch.; Wassermann, B.; Brutschy, B. *Ber. Bunsen-Ges. Phys. Chem.* **1992**, *96*, 1161.
(22) Djafari, S.; Lembach, G.; Barth, H.-D.; Brutschy, B. *Z. Phys. Chem.* **1996**, *195*, 253.
(23) Djafari, S.; Barth, H.-D.; Buchhold, K.; Brutschy, B. *J. Chem. Phys.* **1997**, *107*, 10573.
(24) Huisken, F.; Kaloudis, M.; Kulcke, A.; Laush, C.; Lisy, J. M. *J. Chem. Phys.* **1995**, *103*, 5366.
(25) Weinheimer, C. J.; Lisy, J. M. *Int. J. Mass. Spectrom. Ion. Processes* **1996**, *159*, 197.
(26) Weinheimer, C. J.; Lisy, J. M. *J. Chem. Phys.* **1996**, *105*, 2938.
(27) Lisy, J. M. *Int. Rev. Phys. Chem*. **1997**, *16*, 267 and references therein.
(28) Cabarcos, O. M.; Weinheimer, C. J.; Lisy, J. M. *J. Chem. Phys.* **1998**, *108*, 5151.
(29) Omi, T.; Shitomi, H.; Sekiya, N.; Takazawa, K.; Fujii, M. *Chem. Phys. Lett*. **1996**, *252*, 287.
(30) Hehre, W. J.; Radom, L.; Schleyer, P. von R.; Pople, J. A. *Ab initio molecular orbital theory*; Wiley: New York, 1986.
(31) Ditchfield, R.; Hehre, W. J.; Pople, J. A. *J. Chem. Phys.* **1971**, *54*, 724.
(32) Hehre, W. J.; Ditchfield, R.; Pople, J. A. *J. Chem. Phys.* **1972**, *56*, 2257.
(33) Frisch, M. J.; Trucks, G. W.; Schlegel, H. B.; Gill, P. M. W.; Johnson, B. G.; Robb, M. A.; Cheeseman, J. R.; Keith, T.; Petersson, G. A.; Montgomery, J. A.; Raghavachari, K.; Al-Laham, M. A.; Zakrzewski, V. G.; Oritz, J. V.; Foresman, J. B.; Cioslowki, J.; Stefanov, B. B.; Nanayakkara, A.; Challacombe, M.; Peng, C. Y.; Ayala, P. Y.; Chen, W.; Wong, M. W.; Andres, J. L.; Replogle, E. S.; Gomperts, R.; Martin, R. L.; Fox, D. J.; Binkley, J. S.; Defrees, D. J.; Baker, J.; Stewart, J. P.; Head-Gordon, M.; Gonzarez, C.; Pople, J. A. *Gaussian 94*; Gaussian, Inc.: Pittsburgh, PA, 1995.
(34) Johnson, J. R.; Jordan, K. D.; Plusquelic, D. F.; Pratt, D. W. *J. Chem. Phys.* **1990**, *93*, 2258.
(35) (a) Vinogradov, S. N.; Linnell, R. H. *Hydrogen Bonding*; Van Nostrand Reinhold: New York, 1971; Chapter 3. (b) Joesten, M. D.; Schaad, L. J. *Hydrogen Bonding*; Marcel Dekker: New York, 1974; Chapters 1 and 4.
(36) Fraud, J. M.; Camy-Peret, C.; Maillard, J. P. *Mol. Phys* **1976**, *32*, 449.
(37) Watanabe, H.; Iwata, S. *J. Chem. Phys.* **1996**, *105*, 420.
(38) Xantheas, S. S.; Dunning, T. H., Jr. *J. Chem. Phys.* **1993**, *99*, 8774.
(39) Huisken, F.; Kaloudis, M.; Kulcke, A. *J. Chem. Phys.* **1996**, *104*, 17.
(40) Ebata, T.; Watanabe, T.; Mikami, N. *J. Phys. Chem.* **1995**, *99*, 5761.